TRANSIENT SPARK – DC DRIVEN NANOSECOND PULSED DISCHARGE IN ATMOSPHERIC AIR

Mário Janda[1], Adriana Niklová[1], Viktor Martišovitš[1], Zdenko Machala[1]

[1]*Division of Environmental Physics*
Faculty of Mathematics, Physics and Informatics
Comenius University, Mlynska dolina F2
84248 Bratislava, Slovakia
E-mail: janda@fmph.uniba.sk

We introduce a DC-driven pulsed discharge named transient spark (TS): a repetitive streamer-to-spark transition discharge with short spark duration (~10-100 ns), based on charging and discharging of internal capacity C of the reactor with repetition frequency $f \approx$ 1-10 kHz. TS generates very reactive non-equilibrium air plasma and is applicable for flue gas cleaning, bio-decontamination or other applications, since it can be maintained at relatively low energy conditions (0.1-1 mJ/pulse). Streamer-to-spark transition is governed by the increase of the gas temperature T_g in the plasma channel. Initial T_g at the beginning of the streamer is ~300 K, though it increases with frequency up to ~450 K at 10 kHz. The transition to spark occurs at ~1000 K. This heating accelerates with increasing f, leading to a decrease of the average streamer-to-spark transition time from a few μs to less than 100 ns.

1. Introduction

Atmospheric pressure plasmas in air generated by electrical discharges present considerable interest for a wide range of environmental, bio-medical and industrial applications, such as air pollution control, waste water cleaning, bio-decontamination and sterilization, or material and surface treatment [1-5]. New types of discharges are therefore still being developed and studied, with a focus on efficiency, power requirements, stability, reliability and simplicity [6].

A novel type of transition discharge in air at atmospheric pressure named transient spark (TS) is presented here. TS is a filamentary streamer-to-spark transition discharge initiated by a streamer, which transforms to a short (~10-100 ns) high current (~1-10 A) spark pulse due to the discharging of the internal capacity C of the reactor. TS is based on charging and discharging of C and a repetition frequency of this process from 1 to 20 kHz can be achieved [7].

We observed significant differences between two modes of TS with small and high repetition frequencies [8], studied by time-integrated optical emission spectroscopy. In order to understand the fundamental phenomena related to the evolution of TS and its changes due to increasing repetition frequency, we employed in this study a photomultiplier tube with fast 2.2 ns rise time and appropriate narrow band optical filters, as well as a 2-m monochromator coupled with ICCD camera with 2 ns gate, in order to monitor time evolution of the emission of excited species and of the temperature.

2. Experimental set-up

Experiments were carried out at room temperature in atmospheric pressure air with a radial flow of about 20 cm/s. The distance between stainless steel needle electrode and planar copper electrode (point-to-plane configuration) was 4 mm. A DC High Voltage (HV) power supply connected via a series resistor (R = 6.56-9.84 MΩ) limiting the total current was used to generate a positive TS discharge. The discharge voltage was measured by a high voltage probe Tektronix P6015A and the discharge current was measured on a 50 Ω or 1 Ω resistor shunt. The 1 Ω resistor shunt was used when we focused on TS current pulse itself, whereas the 50 Ω resistor shunt was used to measure current from the streamer. Both voltage and current signals where recorded by a 200 MHz digitizing oscilloscope Tektronix TDS2024.

The emission spectra were obtained using a 2-m monochromator Carl Zeiss Jena PGS2 covering UV and VIS (200-800 nm) and providing spectral resolution of 0.05 nm, cuopled with an intensified CCD camera (Andor Istar). The iCCD camera was triggered by a home-made generator of 5 V rectangular pulses with rise time less than 5 ns. This generator was triggered directly by the current signal, causing

an additional delay of less than 10 ns. This delay, plus the delay caused by the transmission of the signal by BNC cables, was compensated by using 10 m long optical cable (Ocean Optics P400-10-UV-VIS), so that we could see the whole emission profile.
For time-resolved optical emission measurements, a photomultiplier tube (PMT) module with a 2.2-ns rise time (Hamamatsu H955) was also used in place of the monochromator. Its signal was recorded using the oscilloscope. The PMT was triggered by the emission signal itself. Whenever it was necessary to isolate a specific spectral transition for PMT measurements, a band pass interference filter, e.g. Melles Griot 03 FIU127 for the N_2(C-B 0-0) transition, was inserted into the optical path. The experimental set-up is depicted in Fig. 1.

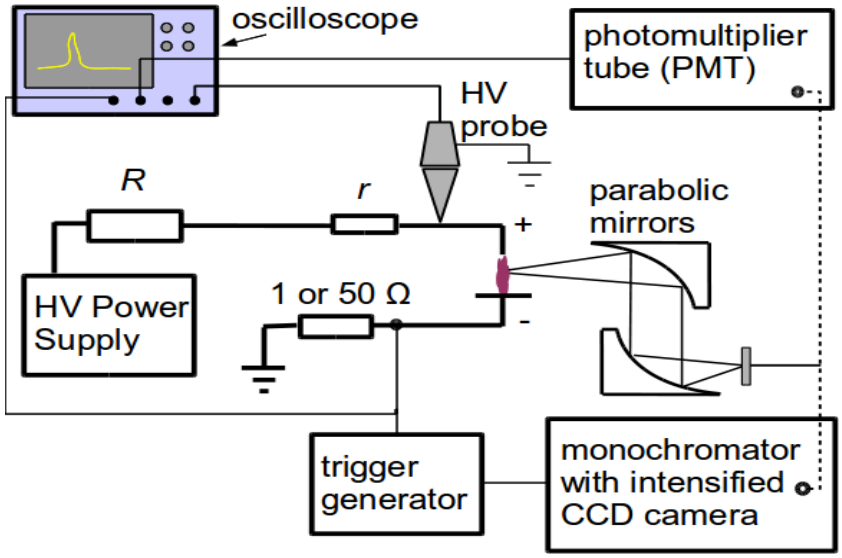

Fig. 1. Schematic of the experimental set-up, HV - high voltage, *R*, *r* - resistors.

3. Results and Discussion

When the high voltage U_{00} applied to the stressed electrode is progressively increased, we first observe a streamer corona. When the breakdown voltage is reached, a transition to TS occurs at the discharge voltage U_{TS}. The typical current and voltage waveforms are shown in Fig. 2a. During the high current phase the voltage drops to zero due to the resistive fall on the ballast resistance *R*. Then, during the quenched phase, the system capacity *C* (composed of the internal capacity of the electrodes, the capacity of the HV cable and of the HV probe) is recharged by a growing potential on the stressed electrode. For typical *R* and *C*, the repetition frequency *f* of this process is in the order of several kHz and grows with increasing U_{00} (Fig. 2b). This is accompanied by changes of TS properties. With increasing *f*, current pulses get smaller and broader (Fig. 3a).

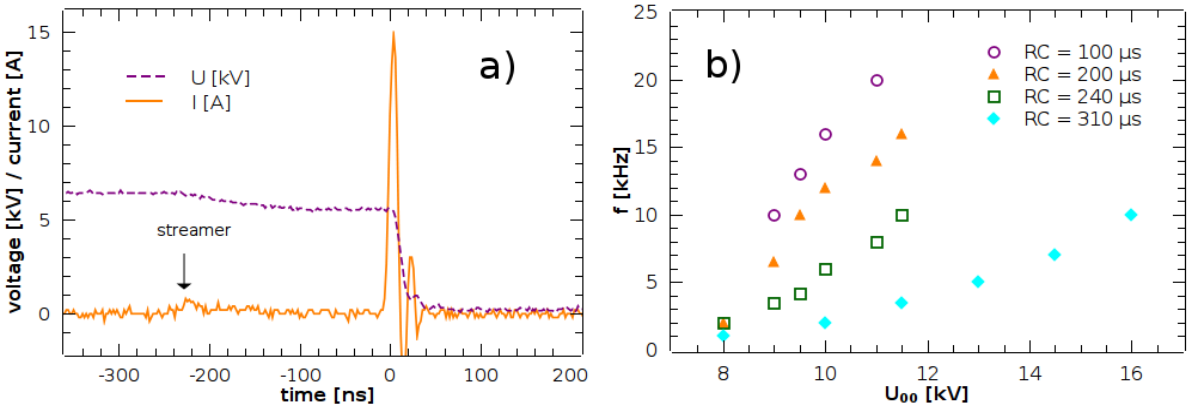

Fig. 2a. Typical TS current and voltage waveform, *f* ~ 1 kHz, *R* = 6.6 MΩ , *C* ≈ 26 pF.
Fig. 2b. The dependence of TS repetition frequency on the onset voltage U_{00}.

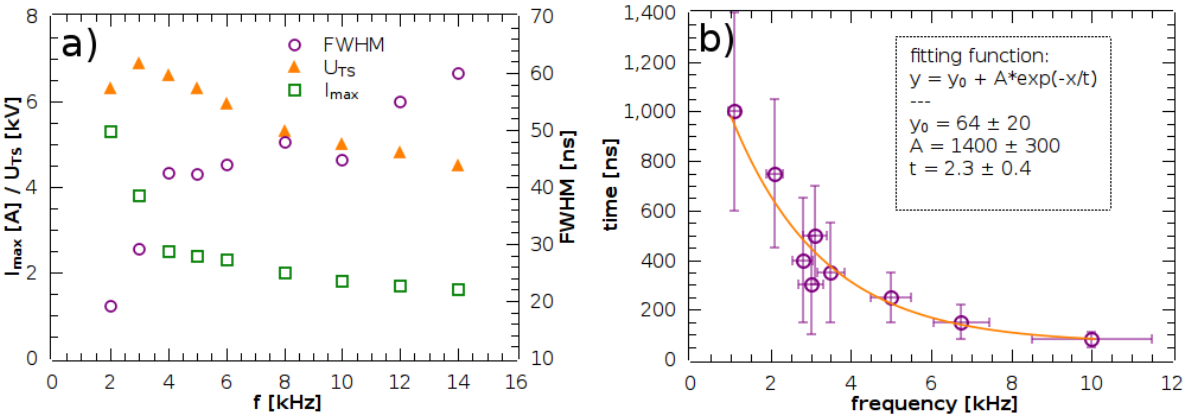

Fig. 3. Dependence of TS properties on f: a) peak current I_{max}, full width at half maximum FWHM of current pulses and breakdown voltage U_{TS}, b) streamer-to-spark transition time, $R = 6.6\,\mathrm{M\Omega}$, $C \approx 26\,\mathrm{pF}$.

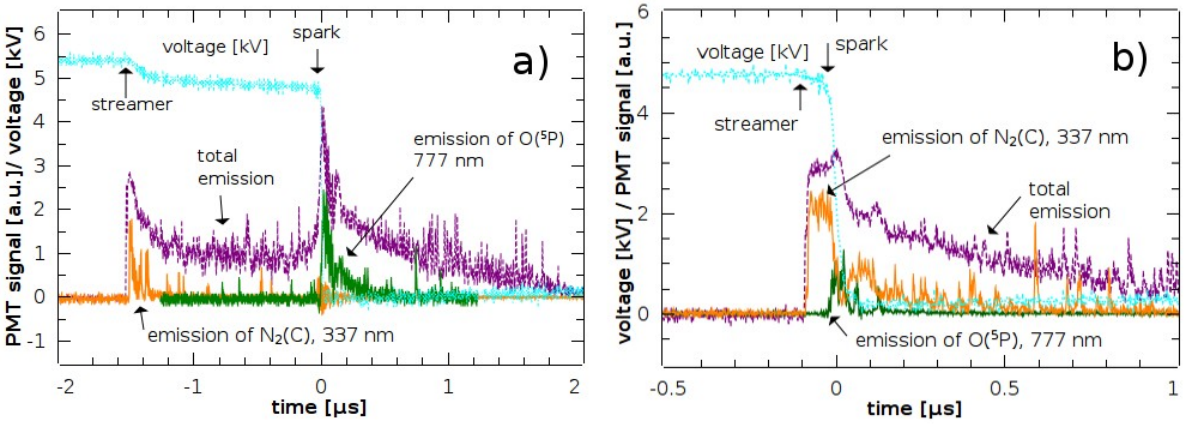

Fig. 4. Typical PMT emission profiles of TS at 2.5kHz (a) and 6 kHz (b), $R = 6.6\,\mathrm{M\Omega}$, $C \approx 26\,\mathrm{pF}$.

It is interesting, that U_{TS} also depends on f (Fig. 3a). The decrease of U_{TS} with f was preliminary explained by the increasing gas temperature T_g, resulting in a decreasing gas density N. Since a certain threshold, the reduced electric field E/N is sufficient to initiate the TS pulse, E and thus also U_{TS} may be lowered [5]. Another reason may be memory effects – the gap remains pre-ionized by previous TS pulses as f increases [7]. Changes of streamer to spark transition time were also observed (Fig. 3b). At lower frequencies (< 2 kHz), the delay between streamer and spark formation is very random and it can vary from several µs to a few hundred ns. As f increases, the average delay time shortens and it becomes more regular.

Significant differences between lower and higher frequency regimes of TS were also observed in time-integrated emission spectra in VIS region. At low frequencies (<3 kHz), the emission of O, N and N^+ atomic lines dominated in the spectra, whereas at higher frequencies these atomic lines almost disappeared and N_2 1st positive system was much stronger. In UV region, N_2 2nd positive system dominated at all frequencies, but its relative intensity compared to atomic lines in VIS region also increased significantly with f. In order to understand this problem, we measured the time evolution of the emission from the strongest atomic line, O(^{5}P) at 777 nm, and from 0-0 band of N_2 2nd positive system at 337 nm by PMT with appropriate interference filters. Figures 4 a) and b) show typical emission profiles at these frequencies, plus the total emission profile at 2.5 and 6 kHz, respectively.

At lower frequencies, we can clearly see two peaks of total emission. The first one is produced by the streamer, whereas the second one corresponds to the short spark. It is obvious, that N_2(C) species are produced mainly during the streamer phase and O(^{5}P) species during the spark phase. The emission profiles also reflect the shortening of the streamer-to-spark delay time with increasing f. The two emission peaks therefore approach to each other and it is difficult to distinguish them at higher f.

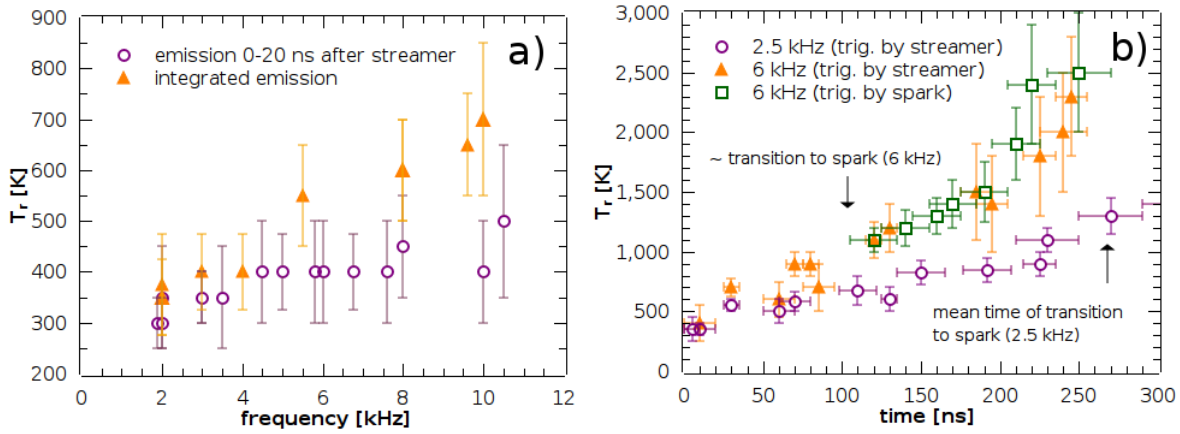

Fig. 5. The rotational temperature T_r of $N_2(C)$ as function of f (a) and time evolution of T_r (b).

The total emission from $N_2(C)$, obtained as an integral of PMT profiles, does not change significantly with f. The reason may be that $N_2(C)$ are mostly produced by collisions of energetic electrons with $N_2(X)$ during the streamer phase of TS and the properties of streamers (E/N, density of electrons n_e) do not change significantly with increasing f. On the other side, the total emission of $O(^5P)$ decreases with f quite significantly. This can be explained by changes of the spark pulse phase of TS with f (Fig. 3a), since $O(^5P)$ are mostly produced during this period. Another possible explanation might be a more complicated mechanism of $O(^5P)$ generation. We suggest the following three step mechanism:

$e + N_2(X) \rightarrow e + N_2(B, C)$ *streamer phase* (1)

$N_2(B, C) + O_2 \rightarrow N_2(X) + 2\,O(^3P)$ *streamer-to-spark transition phase* (2)

$e + O(^3P) \rightarrow e + O(^5P)$ *spark phase* (3)

As the streamer-to-spark transition phase shortens with the growing f, less and less $O(^3P)$ atoms accumulate for the production of $O(^5P)$ during the high current phase by the reaction (3). This does not necessarily mean that the production of $O(^3P)$ decreases significantly with f, it could be just shifted to later phase of TS, after the high current phase. Here, E/N is not strong enough for electrons to gain energy needed to excite $O(^3P)$ to $O(^5P)$. However, we cannot exclude other reactions that could be responsible for the production of $O(^5P)$, e. g. reactions including some metastable species such as $N_2(A)$, $NO(A)$, $O_2(a)$, $O_2(b)$ or $O(^1D)$.

As can be seen in Fig. 4, PMT profiles are quite noisy. The reason is that these emission profiles are from single TS pulses. It was not useful to acquire emission profiles by accumulation of many pulses due to a random character of streamer-to-spark transition. Data from iCCD camera, where the accumulation was necessary, were therefore used mainly for the calculation of rotational temperature T_r of $N_2(C)$ species, obtained by fitting the experimental spectra of N_2 2^{nd} positive system with the simulated ones (using Specair program [9]). We further assumed that in our plasma $T_r \approx T_g$.

Let us explain the reason of the U_{TS} decrease with increasing f from the measured T_r. At the first moment it seems that T_r^{init} calculated from the initial 0-20 ns from the beginning of the emission induced by streamer increases only slightly with f, from about 300 to 450 K, compared to T_r^{total} calculated from time integrated emission of TS (typical integration time 300 μs – 3 ms), which increased to around 700 K (Fig. 5a). However, even this small T_r increase to 450 K is enough to keep an average E/N in the gap about 70 Td when the gap potential at the breakdown voltage U_{TS} decreases from about 7 kV to 4.5 kV (Fig. 3a). The value of T_r^{total} we previously used to describe the increase of T_g with increasing f has actually no physical meaning. To explain it, let us first look at the dependence of T_r on the time from the beginning of the streamer (Fig. 5b).

At both f=2.5 kHz and 6 kHz we observed approximately linear increase of T_r with time, from initial ~300 and ~400 K, respectively. This heating is faster at 6 kHz, but in both cases a streamer-to-spark transition occurs when T_r ~1000 K. We thus suppose that the increase of T_g is a dominant mechanism responsible for the streamer-to-spark transition, leading to the increase of E/N in the streamer plasma column from about 60-70 Td to about ~150-170 Td due to the decreasing N, under an assumption of the constant pressure.

The reason why the delay between the streamer and spark phase shortens with *f* can be explained by a faster growth of T_g with increasing *f*. However, this will require further research and deeper analysis, including kinetic modeling to explain why the growth of T_r accelerates with *f*.
During the spark phase, T_r increases even faster and can reach at least ~2500 K (Fig. 5b), but we were not able to measure it longer than ~250 ns from the beginning of the streamer, because the 2nd N_2 positive signal became too week.
Finally, relatively significant increase of T_r^{total} with *f* can be also explained by a faster growth of T_r with time at higher discharge frequencies. Despite the fact that the whole $N_2(C)$ emission profile contributes to T_r^{total}, we suppose that initial ~100 ns with the strongest intensity dominate. Thus, T_r^{total} represents only something like average T_r during these ~100 ns after the beginning of the streamer emission. At 2.5 kHz, T_r increases to about 600 K during these period, whereas at 6 kHz it is already ~1000 K, which gives T_r^{total} around 400 K and 600 K, respectively. In fact, significant changes of T_r during these ~100 ns also explains large errors of T_r^{total}, despite the signal was strong enough during the measurement of time-integrated spectra. In time-resolved measurements with iCCD gate open for up to 20 ns, the major sources of uncertainties were a weak signal and a random character of TS.

4. Conclusions

We investigated electrical characteristics and time-resolved emission profiles of a DC-supplied periodic streamer-to spark transition discharge in atmospheric air, called transient spark (TS). Thanks to the small internal capacity of the discharge chamber and a limiting series resistor, TS is characterized by the very short spark pulse duration (~10-100 ns) with peak current 1-10 A. TS can be maintained at low energy conditions (0.1-1 mJ/pulse) and generated plasma cannot therefore reach LTE conditions, though the current pulse can lead to temporary increase of temperature to ~2500 K. The global temperature however remains relatively low, since even at repetition frequencies above 10 kHz, each streamer-to-spark process starts at ~450 K.
Subsequent increase of temperature to ~1000 K, accompanied by the increase of the reduced electric field strength inside the plasma channel, governs the streamer-to-spark transition. Shortening of an average streamer-to-spark transition time with increasing TS frequency can be explained by an acceleration of temperature growth. The reason for this acceleration will require further research.
More research is also needed to explain chemical effects of TS. Emission profiles show that streamer is responsible for significant part of the total emission and for almost all emission of N_2 2nd positive system. This proves the importance of streamer in plasma chemistry, but it does not explain why TS was demonstrated more efficient for bio-decontamination than streamer corona. [5] We suppose that during the initial phase of the spark pulse, the strong chemical effect can be maintained thanks to the combination of a relatively strong reduced electric field (>100 Td) and a high electron density.

Acknowledgements

Effort sponsored by the AFOSR, Air Force Material Command, USAF, under grant FA8655-09-1-3110, Slovak grant agency VEGA 1/0293/08 and Slovak Research and Development Agency APVV SK-FR-0038-09.

5. References

[1] Civitano L 1993 Non-Thermal Plasma Techniques for Pollution Control, eds. Penetrante B and Schultheis S E (Springer, New York) NATO Series, Vol. 1, p. 103.
[2] Joshi A A, Locke B R, Arce P, Finney W C 1995 *Journal of Hazardous Materials* **41** 3.
[3] Cernak M et al. 2004 *Contrib. Plasma Phys.* **44** 492.
[4] Pawlat J et al. 2005 *Acta Phys. Slovaca* **55** 479.
[5] Machala Z et al. 2007 *J. Mol. Spectrosc.* **243** 194.
[6] Pai D et al. 2008 *IEEE Trans. Plasma Sci.* **36** 974.
[7] Janda M et al. 2010 *Acta Physica Universitatis Comenianae* **L-LI** 85-93.
[8] Machala Z et al. 2009 *Eur. Phys. J. D* **54** 195.
[9] Laux C O 2002 Radiation and Nonequilibrium Collisional-Radiative Models, von Karman Institute for Fluid Dynamics, Lecture Series 2002-07, Rhode Saint-Genese, Belgium